Developmental Biology 334 (2009) 369–382

Contents lists available at ScienceDirect

Developmental Biology

journal homepage: www.elsevier.com/developmentalbiology

Spots and stripes: Pleomorphic patterning of stem cells via p-ERK-dependent cell chemotaxis shown by feather morphogenesis and mathematical simulation

Chih-Min Lin [a], Ting Xin Jiang [a], Ruth E. Baker [b], Philip K. Maini [b,c], Randall B. Widelitz [a], Cheng-Ming Chuong [a,*]

[a] Department of Pathology, University of Southern California, Los Angeles, CA 90033, USA
[b] Centre of Mathematical Biology, Mathematical Institute, University of Oxford, 24-29 St Giles', Oxford OX1 3LB, UK
[c] Oxford Centre for Integrative Systems Biology, Department for Biochemistry, University of Oxford, South Parks Road, Oxford OX1 3QU, UK

ARTICLE INFO

Article history:
Received for publication 3 September 2008
Revised 22 July 2009
Accepted 27 July 2009
Available online 6 August 2009

Keywords:
Pattern formation
Feather morphogenesis
Stem cells
Placode
ERK
Mathematical modeling
Chemotaxis

ABSTRACT

A key issue in stem cell biology is the differentiation of homogeneous stem cells towards different fates which are also organized into desired configurations. Little is known about the mechanisms underlying the process of periodic patterning. Feather explants offer a fundamental and testable model in which multi-potential cells are organized into hexagonally arranged primordia and the spacing between primordia. Previous work explored roles of a Turing reaction–diffusion mechanism in establishing chemical patterns. Here we show that a continuum of feather patterns, ranging from stripes to spots, can be obtained when the level of p-ERK activity is adjusted with chemical inhibitors. The patterns are dose-dependent, tissue stage-dependent, and irreversible. Analyses show that ERK activity-dependent mesenchymal cell chemotaxis is essential for converting micro-signaling centers into stable feather primordia. A mathematical model based on short-range activation, long-range inhibition, and cell chemotaxis is developed and shown to simulate observed experimental results. This generic cell behavior model can be applied to model stem cell patterning behavior at large.

Introduction

By definition, stem cells are a population of multi-potential or pluri-potential cells. In response to environmental signals they differentiate and assemble into organized tissues and organs. While much has been learned about the molecular signals that induce cell differentiation (Keller, 2005), less is known about the rules that govern their morphogenesis. This is vividly illustrated in the case of pluri-potential embryonic stem cells, as seen both in the differentiated, yet unorganized, embryoid body and in teratoma. Attempts to engineer multi-potential stem cells into organs have found the requirement for architecture diminished when stem cell products are released into the bloodstream (which does not require structural organization), as seen in bone marrow stem cells (Weissman, 2000). However, it becomes an acute issue when the architecture of the stem cell product is critical to its function, as is the case for skeletal regeneration and engineered hair follicles (Watt, 2001; Widelitz et al., 2006). Progress in the tissue engineering of stem cells has pushed this issue beyond basic interest and realm of practical ramifications. While analytical approaches have provided valuable data enabling us to identify, for example, essential molecules for morphogenetic processes, the rules that govern spatial patterning remain elusive. We now need to pursue a systematic approach to comprehend how these molecular pathways work together to build the architecture of a tissue/organ (Chuong et al., 2006).

One of the most fundamental processes in molding organ architecture is the ability of cell populations to form periodically arranged spots and stripes (Fig. 1A). These patterns are striking when they are observed in the integument pigment pattern of leopards, tigers, fishes, etc., (Wolpert, 1971; Ball, 1999; Kondo, 2002), the segmented vertebrae (Dequéant and Pourquié, 2008), and skin appendage arrangement (Jiang et al., 2004). Theoretical models have been proposed to explain these phenomena (Liu et al., 2006; Murray, 2003; Maini et al., 2006; Meinhardt and Gierer, 2000). Some developmental systems may be based on combinatorial molecular coding which can be interpreted at the enhancer/transcription factor level (e.g., Drosophila segments; Small and Levine, 1991). Others may be based on molecular oscillations and wave fronts (e.g., somitogenesis; Pourquie, 2003). It is likely these complex patterning processes may involve epigenetic, stochastic, and self-organizing processes (Newman and Comper 1990; Jiang et al., 2004; Newman et al., 2008; Christley et al., 2007). Mechanisms involving the reaction and diffusion of chemical substances and the chemotactic response of cells to such chemicals have been proposed for a number of biological phenomena including the pattern-forming behavior of the slime

* Corresponding author. HMR 313B, Department of Pathology, Keck School of Medicine, University of Southern California, 2011 Zonal Avenue, Los Angeles, CA 90033, USA. Fax: +1 323 442 3049.
E-mail address: cheng-ming.chuong@keck.usc.edu (C.-M. Chuong).

0012-1606/$ – see front matter © 2009 Elsevier Inc. All rights reserved.
doi:10.1016/j.ydbio.2009.07.036

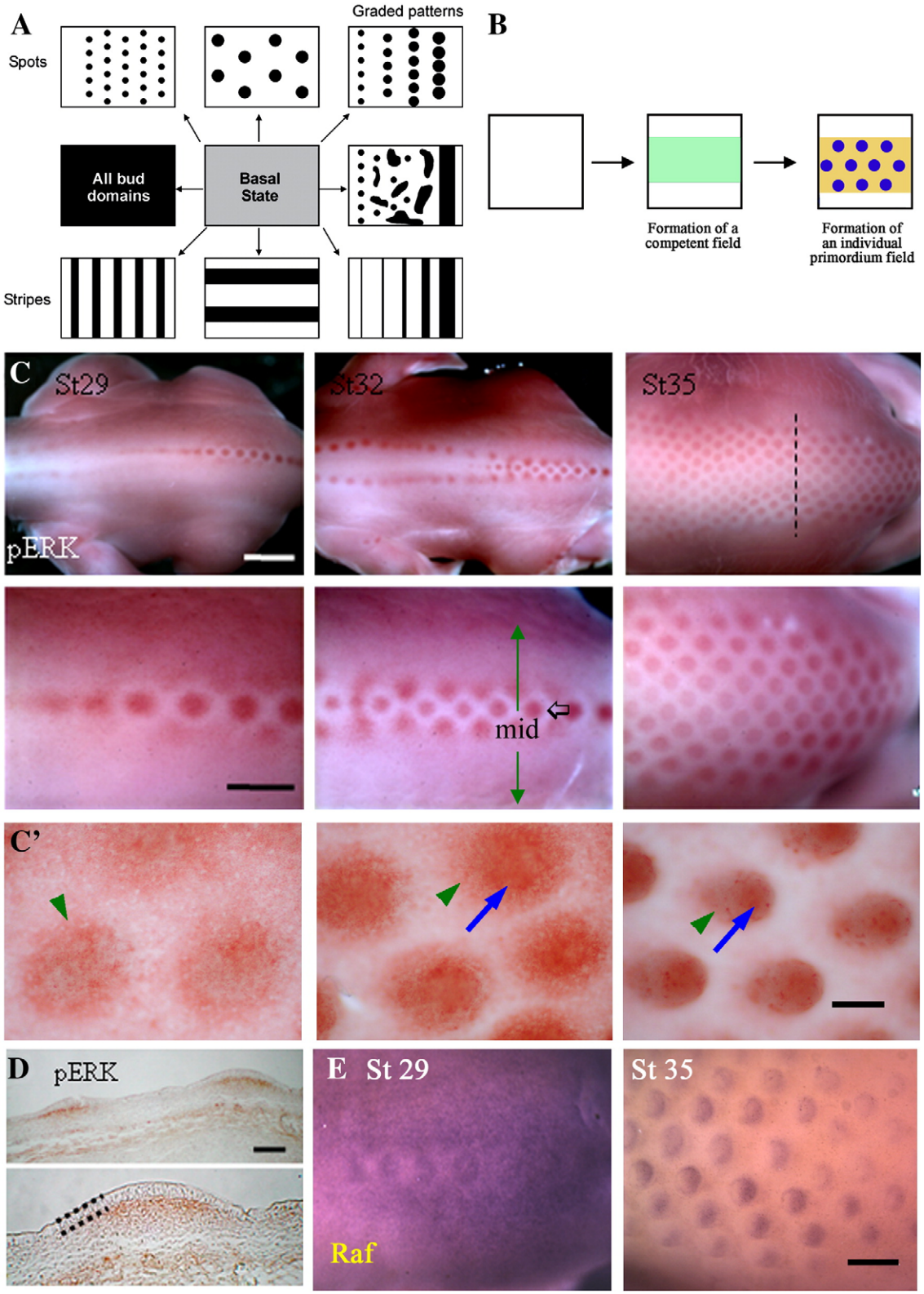

Fig. 1. Expression of p-ERK and related molecules. (A) Schematic drawing highlights the fundamental question of generating different distributions of bud (black) and interbud (white) zones forming spots or stripes of different number and sizes and spacing from a homogeneous basal stem cell state (grey) in response to chemotaxis. (B) Schematic drawing showing the emergence of a competent feather tract field (green) and its conversion into bud (blue) and interbud states (yellow) in response to chemotaxis. (C) Whole-mount immunostaining shows expression of phosphorylated ERK at different feather development stages. Staining marks the feather placodes which initiate along the dorsal midline at stage 29 and spread bilaterally from the midline (black arrow) with developmental progression (green arrows). Scale bar is 2 mm in the upper row, and 1 mm in the lower row. (C′) High power view of p-ERK in different stages of feather buds. p-ERK is first expressed in a wider region and at a medium level. Then p-ERK becomes enriched in the central bud domain (blue arrow) while the peripheral expression (green arrowheads) gradually decreases. Scale bar is 100 μm. (D) Section from a stage 35 embryo. The section plane is shown as the dashed line in panel (C). A dotted line marks the epithelium of the feather bud. Staining is present in the mesenchyme beneath each feather placode. Scale bar, 0.15 mm. (E) Raf expression at stages 29 and 35 shown by whole-mount *in situ* hybridization. Expression is initially throughout the morphogenetic field and becomes progressively restricted to the posterior feather bud by stage 35. Scale bar, 300 μm.

mold, *Dictyostelium discoidium* (Vasiev et al., 1994) and the bacterium *E. coli* (Zorzano et al., 2005), patterns on the integument of snakes and fish (Myerscough and Murray, 1991; Painter et al., 1999), in the induction of hairs and feathers (Nagorcka and Mooney, 1992; Jung et al., 1998) and feather branching (Harris et al., 2005; Yu et al., 2002). These principles also have been used to explain skeletal patterning in the limb bud (Hentschel et al., 2004; Kiskowski et al., 2004; Miura and Maini, 2004). However, much remains to be learned about how molecular pathways and cellular events are coupled to the patterning process at the tissue/organ level.

The periodically arranged feather arrays on embryonic chicken skin (Fig. 1B; Lin et al., 2006) provide an excellent paradigm for studying this issue. In the feather, at the outset, both epithelia and mesenchyma are homogenous, *i.e.*, every cell is multi-potential and has an equal probability of becoming bud or interbud (equipotent), as demonstrated by DiI labeling in a reconstitution experiment (Chuong et al., 1996; Jiang et al., 1999). When feathers start to form, this homogeneity is disrupted, leading to the emergence of new arrangements or structures. In the chick, feathers arise in a sequential manner, from the dorsal midline out to the lateral regions (Fig. 7). The exquisite two-dimensional layout makes it easier to see experimentally driven alterations in feather arrangements. Skin epithelium and dermis recombination experiments show that the initial patterning signal arises from the mesenchyme (Sengel, 1976). However, the molecular networks and mechanisms involved in establishing the periodic pattern remain elusive. Experimental work has shown that members of the FGF family, such as FGFs 1, 2, 4, as well as noggin and follistatin, function as activators by promoting feather bud formation (Jung et al., 1998; Song et al., 1996, 2004; Patel et al., 1999; Widelitz et al., 1996). On the other hand, the BMPs and Delta-1 function as inhibitors by suppressing bud formation (Jung et al., 1998; Noramly and Morgan, 1998; Crowe et al., 1998; Viallet et al., 1998). Since gene networks are likely to drive the complex patterning process, tilting the balance of activator or inhibitor concentrations may result in different feather patterns (Chang et al., 2004; Jiang et al., 2004).

While activators and inhibitors are involved in the spatial patterning of skin precursor cells (Jung et al., 1998; Sick et al., 2006), exactly how molecular events combine to produce the feather primordia array is unclear. We have previously proposed that the interaction of activators and inhibitors could lead to a stable chemical concentration pattern. However, a reaction–diffusion mechanism alone is not sufficient to account for the changes in cell density which lead to the progression from a homogeneous field to small cell clusters and, finally, to committed stable dermal condensations (Jiang et al., 1999). In addition, the complexity of the patterning process is further highlighted by the dramatically different phenotypes obtained when the timing of signal pathway perturbation is subtly altered (Widelitz et al., 1996; Drew et al., 2007). Therefore, with our current, novel observations we propose that, along with the reaction and diffusion of activators and inhibitors, a cell-chemotaxis mechanism is required to achieve mesenchymal condensation and complete the periodic pattern-forming process.

As mentioned previously, FGFs are involved in feather pattern formation (Song et al., 1996, 2004; Mandler and Neubuser, 2004; Widelitz et al., 1996). FGFs 1, 2 and 4 can induce many smaller feather buds from embryonic chicken skin explant cultures (Widelitz et al., 1996) and induce dermal condensations (Song et al., 2004). On the other hand, FGF10 induces epidermal thickening and enlarges feather primordia while decreasing the number of feather buds (Tao et al., 2002). The addition of dominant negative soluble FGFRs 1 and 2 at an early developmental stage inhibits feather bud formation (Mandler and Neubuser, 2004). FGFR1 is expressed initially beneath the feather placode and subsequently in the anterior feather bud mesenchyme. FGFR2 is expressed in the mesenchyme between the feather placode and the ectoderm of feather buds. On the other hand, FGFR3 expression is more ubiquitous (Noji et al., 1993). In scaleless mutant skin, beta-catenin is induced in the track field, but fails to form periodic patterns (Widelitz et al., 2000), while FGF can rescue feather bud formation in the skin of embryonic scaleless mutant chickens (Song et al., 1996; Viallet et al., 1998). These results imply an essential role for FGF in epithelial–mesenchymal interaction during feather morphogenesis. However, how it works at the cellular level remains unknown.

FGFs exert their effects through the Raf-MEK-ERK pathway in a number of developmental systems (Cabernard and Affolter, 2005; Delfini et al., 2005; Fisher et al., 2001; Matsubayashi et al., 2004; Sawada et al., 2001). Here we show that FGF-ERK activity plays a role in controlling the migratory behavior of cells observed during the dermal condensation process, which helps to transform a homogeneous field of feather precursor cells into discrete cellular condensations. Adding inhibitors of ERK phosphorylation to pattern-forming explant cultures produces a spectrum of placode patterns ranging from broad stripes when added early in placode formation to anastomosing, segmented stripes and spots when added later. We propose that these stripes and spots represent a continuum of equilibrium states of morphing dermal condensations during the patterning process (Fig. 6A). To gain a global understanding, we develop a mathematical model with cell movement driven by chemotaxis towards areas containing high chemo-attractant concentrations. We show that chemotactic movement toward initial chemo-attractant concentration peaks is essential for stabilizing the bud pattern and that this process requires ERK signaling in the mesenchyme (Fig. 7; Supplementary movies 6–8). The mathematical formulation of our model can reproduce the experimentally observed results and predict cell behavior. This study integrates theoretical and experimental approaches and opens new avenues of research in patterning stem cells.

Results

ERK is specifically phosphorylated in feather buds during the periodic patterning process

In the spinal tract, feather formation begins with the development of a primary row of buds along the midline. The primary row initially forms as a stripe, as visualized by the molecular expression of several molecules, which contains an initiation point for feather formation. This serves as the point of convergence between stripes and spots (feather buds). After the primary row of feather buds form, a morphogenetic patterning wave propagates bilaterally to establish the lateral rows. FGFs and FGFRs are expressed in a restrictive mode (initially expressed all over, becoming restricted to the bud region; Widelitz et al., 2000) in the forming feather primordia (Jung et al., 1998; Song et al., 1996; Mandler and Neubuser, 2004; Tao et al., 2002; Widelitz et al., 1996). Here we focus on the intracellular signaling events downstream of the FGFs. To study the involvement of MAPK/ERK signaling, the phosphorylated form of ERK was examined in stages 28 and 35 skin using whole-mount immunostaining. Along the primary row, buds progressively form in a posterior to anterior direction. p-ERK is first homogeneously expressed in the morphogenetic zone (the periodic pattern-forming region; Jiang et al., 1999). It then becomes restricted to the bud region, with a surrounding clear, lateral, halo-shaped inhibition zone, and finally it segregates into periodically arranged buds (Fig. 1C). A high power view shows that at the feather placode stage, there are medium levels of p-ERK present distributed in a diffuse way. At the short bud stage, medium levels of p-ERK are still present, but a central domain with high p-ERK expression starts to appear (Fig. 1C′). In the long bud stage, strong expression is restricted to the bud region, while the interbud region becomes deficient of p-ERK, establishing a distinct boundary between the two. This is typical of the restrictive mode of expression. Sections show p-ERK staining in the mesenchyme (Fig. 1D). Expression of Raf, an upstream ERK pathway member, was assessed by *in situ* hybridization. It also shows

a restrictive mode expression pattern: first expressed throughout the morphogenetic field at stage 29, then becoming progressively restricted to the feather buds. Later, at stage 35, Raf expression becomes further restricted to the posterior feather bud (Fig. 1E). Raf is also expressed in both the epithelium and mesenchyme (Widelitz et al., 1996).

Suppressing p-ERK activity leads to a range of stripe patterns

To test the role of p-ERK, we first perturbed p-ERK pathways using siRNA targeted suppression of ERK transcripts. Skin explants were electroporated with siRNA-ERK or a scrambled siRNA (control) sequence. CMV-RFP was co-electroporated to enable identification of the affected regions. Results showed feather buds appear as short anastomosing stripes and merged plateaus (Fig. 2A).

To manipulate the level of p-ERK more effectively, we used a chemical inhibitor of ERK phosphorylation. Western blot analysis showed that U0126 reduces p-ERK levels in skin explants (Fig. 2B). When U0126 was added to stage 31 skin explants, the feather patterns changed in a dose-dependent manner (Fig. 2C). At low dosage (2.5 mg/ml or 6 μM), feather bud elongation was inhibited. The diameter of the bud base expanded while the interbud spacing diminished. At a high dosage (10 mg/ml or 25 μM), the buds fused into stripes. At the highest dosage (20 μg/ml), feather bud formation was completely inhibited. The feather buds were all fused together to form broad stripes.

Inhibition of p-ERK in the presence of U0126 was verified by whole-mount immunostaining for p-ERK using Rabbit anti-p-ERK antibodies. This showed that p-ERK was expressed in feather bud regions and was gradually reduced in explants treated with 2.5 and 10 μg/ml of U0126. In explants treated with 20 μg/ml of U0126 (or 50 μM), p-ERK expression was totally suppressed (Fig. 2D). Thus there is a U0126 dose-dependent reduction of ERK phosphorylation levels that correlates with the gradual morphological transformation from spots to stripes.

The feather explant culture system provides an excellent opportunity to observe the consequences of suppressing p-ERK at different time points. Since feather buds first form in the posterior midline, then anterior midline, and later the lateral regions of the explants (Fig. 6A. schematic bird drawing), different parts of stage 28 and 31 explants can actually represent different time periods from early to late development. Specifically, we consider that the lateral region of a stage 28 explant, mid-region of a stage 28 explant (Fig. 3C), lateral region of a stage 31 explant and mid-region of a stage 31 explant (Fig. 3B) represent different stages of feather development. If suppression takes place very early, as in the lateral region of a stage 28 explant, formation of the bud domain is entirely inhibited. The explant forms broad sheets which gradually break into long stripes towards the midline. Long stripes can be seen in the lateral region of a stage 31 explant. Towards the midline, these stripes further break into anastomosing stripes, and eventually become short stripe segments and some discrete buds. Thus, these stripes and spots represent a spectrum of patterns when the dermal condensation process is abolished at different times. Similar altered patterns can also be observed in the control (Figs. 4A and 5A). Short "bud stripes" resemble those observed on skins treated with the DN FGFR (Mandler and Neubuser, 2004).

To test the reversibility of the effect of U0126, we cultured skin explants in the presence of U0126 for two days. U0126 was then washed away, and the explant continued to be cultured for two or four

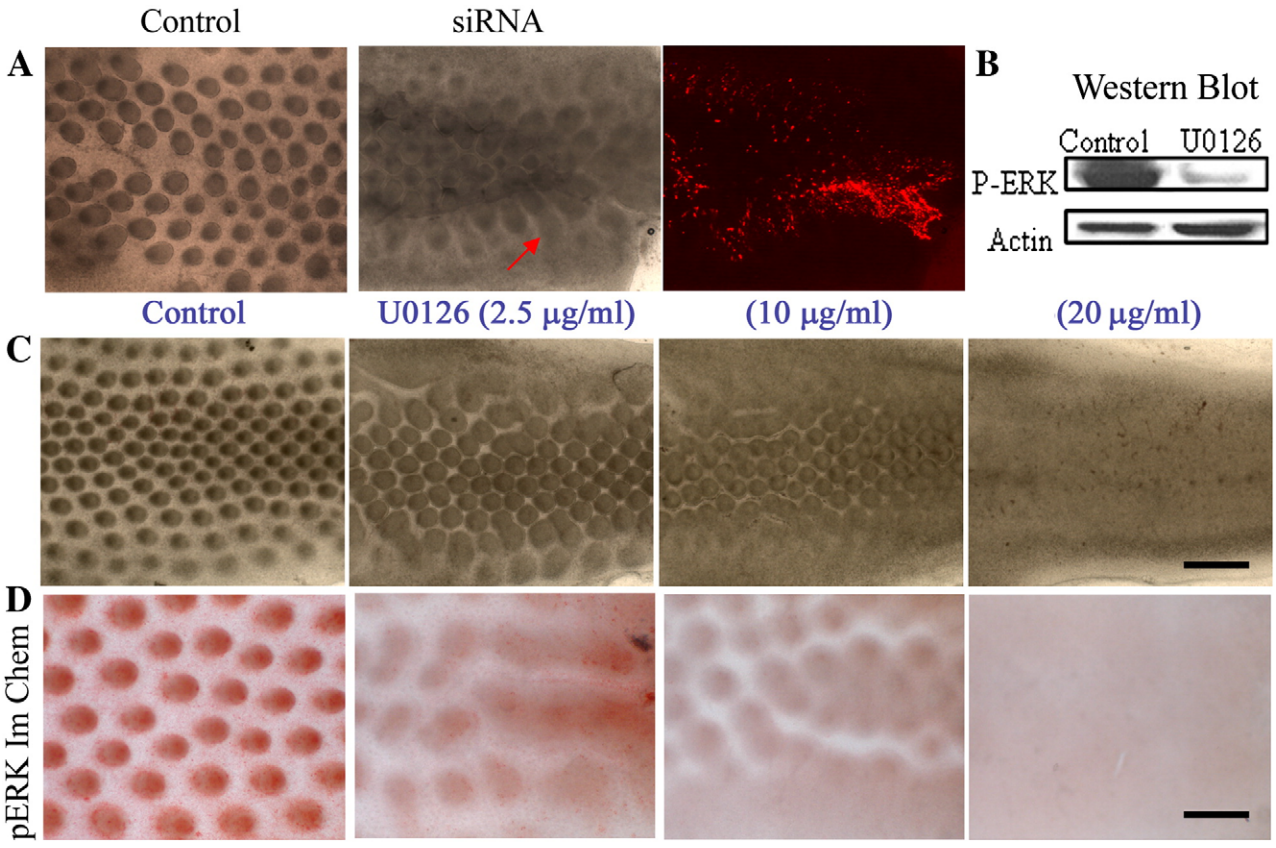

Fig. 2. Converting spots to stripes by suppression of the ERK pathway. (A) Stage 30 skin explants were electroporated with random siRNA or siRNA-ERK. After two days of culture, those with siRNA-ERK showed a failure to form distinct feathers buds, but the skin formed stripes and raised plateaus. RFP was co-electroporated with siRNA-ERK to show the distribution of siRNA. (B) Western blot shows that p-ERK expression is almost completely absent after U0126 treatment. (C) Effect of U0126. Control (DMSO), U0126 at 2.5, 10 and 20 μg/ml showed that U0126 gradually converts spots to strips in a dose-dependent manner. Scale bar, 500 μm. (D) Samples in (C) are immuno-stained with antibodies to p-ERK. There is a parallel conversion from spots to stripes and reduction of p-ERK expression. Each of these experiments was performed in triplicate. Size bar = 300 μm.

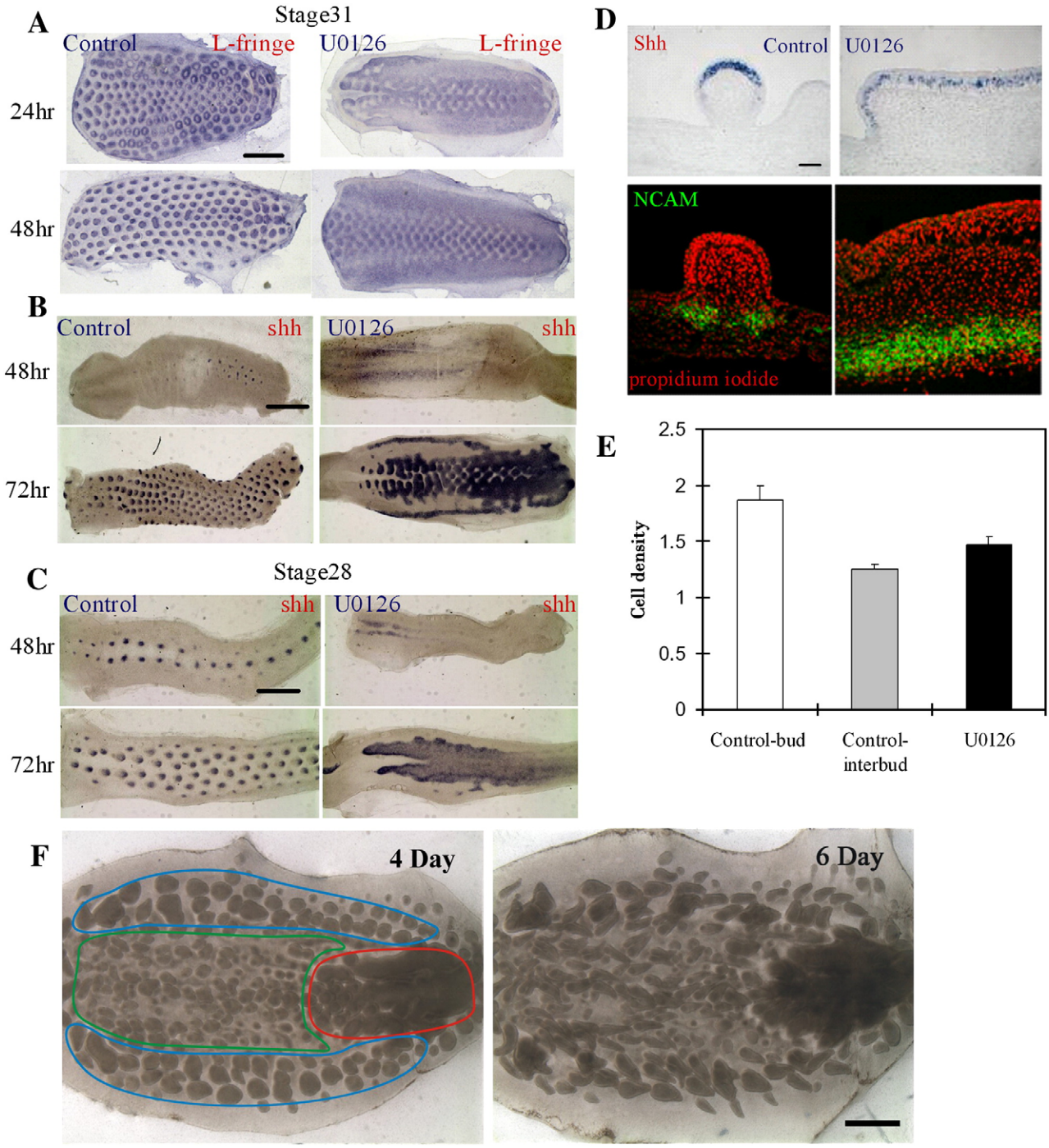

Fig. 3. Molecular expression of the stripes caused by inhibition of ERK signaling. (A–C) Whole-mount *in situ* hybridization. Time course studies of stage 28 and 31 explant cultures are shown in Supplementary Figs. B, C and Movies 1–4. (A) The expression pattern of L-fng becomes localized to the buds and further polarized in control skin explants. When stage 31 skin is treated with U0126, L-fng remains diffuse. Scale bar, 2 mm. (B) In the control, Shh appears in each feather bud placode through the *de novo* expression mode. When U0126 is added at stage 31, Shh is expressed as spots in the middle rows (more mature), but as stripes (less mature) in both lateral sides of the explant. (C) When U0126 is added at stage 28, Shh is expressed in the whole feather field as the feather primordia are still in early morphogenetic stages. Scale bar, 2 mm. (D) Section *in situ* hybridization shows that Shh is expressed throughout the whole stripe epithelium in ERK inhibited skin. Immunostaining: the dermal condensation marker, NCAM is expressed throughout the mesenchyme of the fused feather. Each of the above experiments was performed in triplicate. (E) Cell densities in the bud, interbud and stripe regions are shown with standard deviation. They were determined by cutting and staining sections with the nuclear stain, propidium iodide. Cells were counted from 3 sections representing each experiment for 5 independent skin explants. (F) Irreversibility of U0126. Stage 30 skin explants were cultured for one day in the presence of 10 μg/ml U0126. The explant was then washed clean of U0126 and was cultured for 5 days without U0126. The same explants were photographed after three more days (marked as total 4 days in culture), or 5 more days (marked as total 6 days in culture) of culture. Red, green and blue contour lines delineate the regions with distinct morphology because they are before (blue), during (green), or after (red) the periodic patterning process during the two days of U0126 exposure.

more days (Fig. 3F). The temporal sequence of skin maturation from posterior midline, anterior midline to lateral flank regions was investigated (Fig. 3F, the red, green and blue regions, respectively). If the region has already formed feather primordia when it encounters U0126, the feather primordia cannot continue to attract dermal cells to form distinct dermal condensations, and therefore a broad area of stripes form (Fig. 3F, red region). If the region is in the middle of the periodic patterning process when it encounters U0126, many small

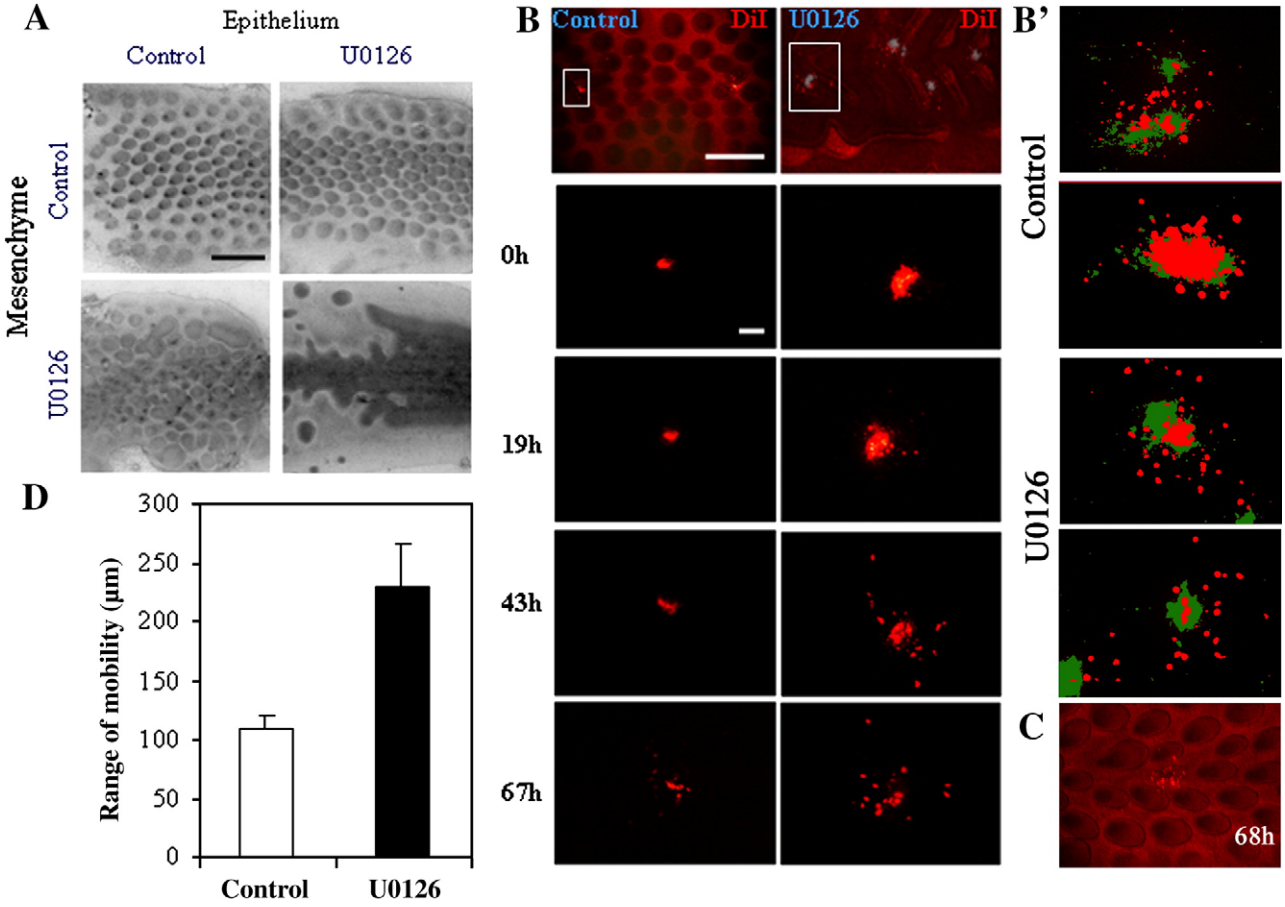

Fig. 4. Involvement of p-ERK signaling in mesenchymal condensation. (A) Skin recombination studies treating epithelium or mesenchyme with U0126 show that the pattern is mediated primarily by the mesenchyme. However, the phenotype is even more severe when both U0126-treated epithelium and mesenchyme are recombined. These studies were performed in quadruplicate. (B) DiI was injected directly into regions of the mesenchyme in control (left column) or U0126-treated skin (right column) explants at stage 35. Injection sites are marked with a gray color. Cell migration within the indicated rectangle (upper panel) is tracked over time. Cells in U0126-treated skin show a much larger range of cell motility. At least 10 regions were followed from each of 10 skins for the DiI migration studies. (B′) Next we injected DiI randomly into the bud and interbud regions of the skin mesenchyme at stage 30 to compare cell motility within both regions. Here the DiI distribution immediately after injection ($T=0$; green) or after 68 h ($T=68$ h; red) are shown. The photograph of 68 hour explants was placed above the 0 hour photograph to visualize cell migration. While migration does not occur uniformly in all directions, the U0126-treated cultures show greater distance of cell migration in both bud and interbud regions. In both control and UO126, two independent specimens are shown. (C) The bottom panel shows that when bud cells are labeled in early bud stage, we can see some bud cells can migrate into the interbud region without UO126 treatment. (D) Over the 67 h dermal condensation period, the average distance traveled by cells in U0126-treated dermis is about two-fold higher than that of the control. Size bar in A, 2 mm, B, 200 μm.

buds form as the dermal condensation processes that are supposed to continue to build up bigger buds are now blocked (Fig. 3F, green region). If the region has not started the periodic patterning process when U0126 was present, and started patterning after U0126 was removed, then the pattern is not affected (Fig. 3F, blue region). Thus, differences in temporal competence are revealed as different phenotypes in different explant regions. Furthermore, the phenotypes, once formed, are stable as seen in the explant after either 2 or 4 days of culture (Fig. 3F, right panel). Thus the effect of U0126 on the periodic patterning of feather buds is irreversible.

Molecular characterization of the stripes

What is the differentiation status of these stripes? Can they be considered as equivalent to an interbud region, are they a tract field which cannot progress, or do they represent giant, fused buds? We examined molecular expression patterns to help interpret these findings. We tested both restrictive and *de novo* mode signaling molecules, using L-fringe (L-fng) and Sonic hedgehog (Shh) as representatives, respectively. When stage 31 skin was cultured for one day, L-fng was present in the periodically arranged array, in either a circular or posterior configuration, representing its expression patterns at different developmental stages (Chen and Chuong, 2000). At day two, in the presence of U0126, the medial rows form buds which fuse laterally to form short "bud stripes". The lateral rows are still in the early morphogenetic stage with unsegregated L-fng staining (Fig. 3A). Notch has similar expression patterns (not shown). Shh showed weak staining at day two. At day three, Shh appeared in the short horizontal bud stripes which form in the midline region, and in the two long longitudinal stripes which form at the lateral edges of the explants (Fig. 3B). An inter-stripe region is present between them. When stage 28 explants were used, a wider and more homogeneous stripe appeared with homogeneous Shh expression (Fig. 3C).

Tissue sections showed that the placode marker, Shh, is diffusely present at a low level in the stripe epithelia (Fig. 3D). β-catenin is expressed but also at lower levels than in control bud epithelium (not shown). The epidermis is thickened (Fig. S1D and Fig. 3D), but remains unpatterned. The dermal condensation marker neural cell adhesion molecule (NCAM) is expressed periodically at the base of individual buds (Jiang and Chung, 1992), but in a continuous and diffuse layer of dermal cells in the fused bud mesenchyme (Fig. 3D, H&E staining of these sections is shown in Fig. S1D).

Cell density in bud, interbud and striped regions was quantified. From homogeneity, cell density becomes mosaic-like: high ($1.86\pm 0.13/100\ \mu m^2$) in the bud and low ($1.24\pm 0.04/100\ \mu m^2$) in the interbud regions (Sengel, 1976; Fig. 3E). The striped region showed an average cell density of $1.47\pm 0.07/100\ \mu m^2$ (Fig. 3E), suggestive of a plateau state somewhere between the bud and basal state (Fig. 7).

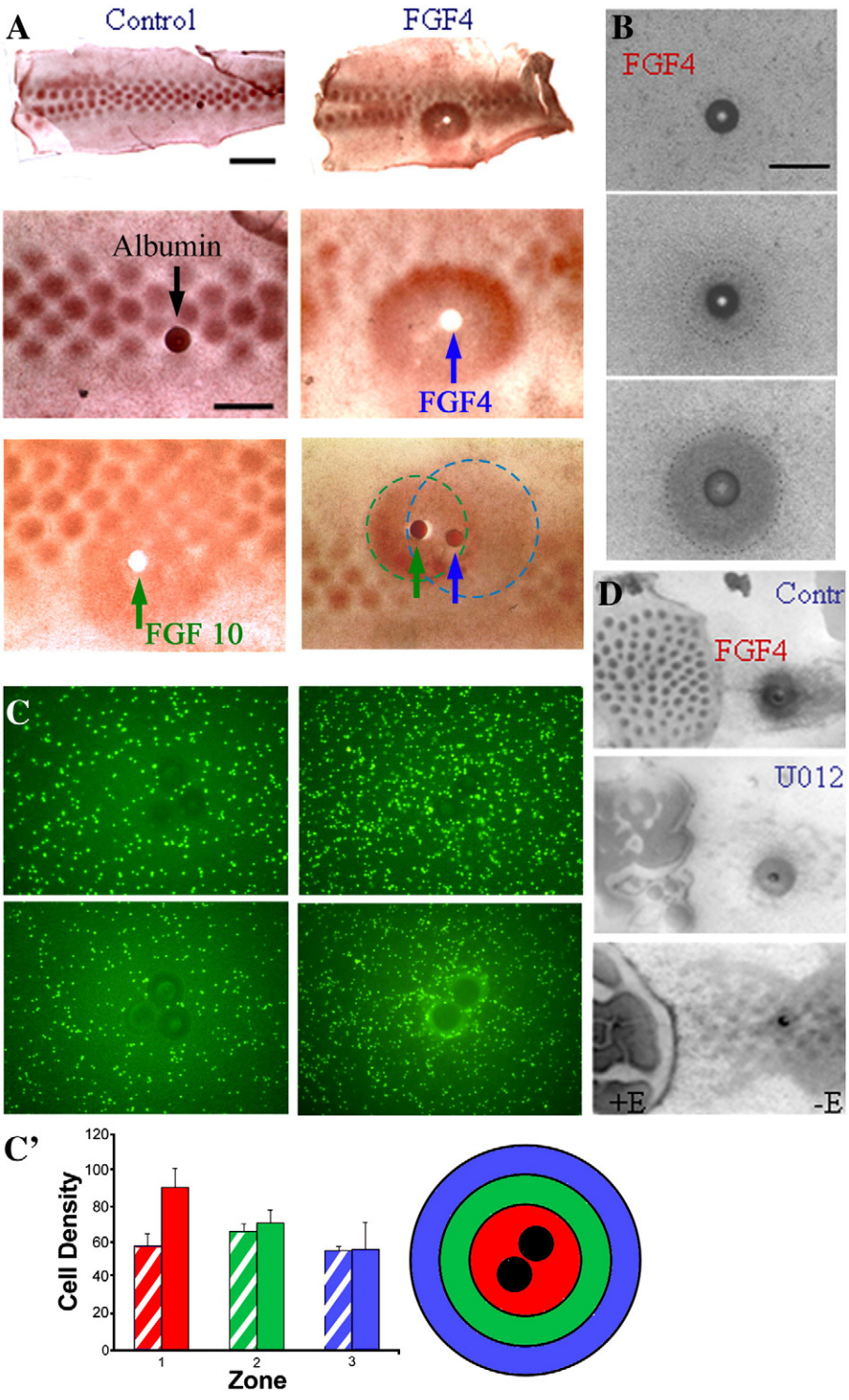

Fig. 5. Involvement of FGF in p-ERK dependent chemotactic cell migration. (A) FGF4-coated beads (blue arrow, shown as a white spot because the bead was displaced during processing) placed on stage 31 skin explants induced p-ERK expression (brown staining) after 4 h that was not seen in explants incubated with control beads (dark spot, upper panel scale bar is 2 mm and lower panel is 1 mm). FGF10-coated bead (green arrow) has similar effects as FGF4. When FGF4- and FGF10-coated beads are placed side by side, the region of p-ERK expression is wider (additive), but the level of p-ERK expression is not higher (non-additive). The expected region affected by the growth factors and their possible regions of overlap are indicated by the dotted lines (FGF4, blue; FGF10, green). (B) On the denuded mesenchyme, FGF4-induced mesenchymal condensation formation during 0 to 20 h. A time lapse movie (Supplementary movie 5) shows that mesenchymal cells are attracted to the FGF4-coated bead. (C) FGF4-coated beads were placed on dissociated mesenchymal cells (density of 1×10^6 cells/10 nl) that were stained with Vybrant CFDA SE Cell Tracer (10 mM; Invitrogen, Carlsbad, CA, USA). FGF4 induced the mesenchymal cells to migrate towards the FGF4-coated beads over time. Cells did not migrate towards control beads. Times shown are 0 (left panel) and 26 h (right panel). (C′) The average of 5 independent replicate experiments from (C) +/− SD are graphed with standard deviations to show the accumulation of labeled cells near the bead (red region) but not at progressively greater distances (locations 2 and 3) from the bead (green and blue regions). Hatched, control bead; solid color, FGF 4 bead. (D) In the presence of U0126, the ability of an FGF4-coated (100 μg/ml) bead to induce dermal condensations from the mesenchyme. Top panel, an FGF4 bead can induce dermal condensations from denuded mesenchyme. Middle, this ability of FGF4 is reduced in the presence of U0126. Bottom panel, chemotaxis towards a bead with a lower concentration of FGF4 (5 μg/ml) is totally abolished by U0126. Left: with epithelium (+E) as control. Right: without epithelium (−E). Each experiment was performed in triplicate. Scale bar, 1 mm.

p-ERK activity is required for dermal condensation

E30 chicken skin was cultured with or without 25 μM U0126 for 16 h and the epithelium and mesenchyme then separated after 2× CMF + 0.25% EDTA buffer incubation on ice for 10 min. The separated epithelium and mesenchyme were then recombined in different ways (Fig. 4A). As the effect of U0126 on bud morphogenesis is irreversible (Fig. 2F), we can now determine whether the action of U0126 is more dependent on epithelium or mesenchyme. U0126-treated or non-treated epithelia and mesenchyme were recombined, and the chimeric explants were cultured for two more days. U0126-treated epithelium recombined with non-treated mesenchyme resembled control feather arrays. In contrast, control epithelium recombined with U0126-treated mesenchyme caused the formation of short stripes, co-existing with discrete primordia. The phenotype was more severe when U0126-treated epithelium was recombined with U0126-treated mesenchyme.

To test the effects of FGF4-ERK signaling on cell migration, we used DiI to track cell motility (Fig. 4B). DiI was injected directly into the mesenchymal side of skin explants, labeling different mesenchymal cell regions. The original labeled spot was about 150–200 μm in diameter. The location of the DiI was determined at 0, 19, 43 and 67 h (Fig. 4B). In a period of 67 h, cells migrated 109.5 μm ± 11.5 μm in control skin and 231 μm ± 34.6 μm in U0126-treated skin (Fig. 4D). Therefore, there is a tendency in the control skin for cell movement to be condensed toward each bud. When the MAPK pathway is suppressed, cells scatter over a much wider range, implying a failure of the dermal condensation process. An interesting observation is that cell movement in the treated skin tends to be along the anterior–posterior axis, consistent with the stripes formed near the midline.

Next we applied DiI to stage 30 embryonic skin, in both bud and interbud mesenchyme to determine whether migration differed between these two regions. We injected the mesenchymal regions of ten control and ten U0126-treated skin explants and cultured them for 68 h. The location of DiI was photographed at 0 (green) and 68 h (red). We then overlaid the red photograph over the green photograph to visualize how far the cells migrated over this period of time (Fig. 4B′). Mesenchymal cells did not migrate uniformly in all directions but in each example DiI labeled cells migrated further in U0126-treated skin. Both bud and interbud regions showed increased migration after U0126 treatment.

The degree of mesenchymal cell migration seen in B′ implies unstable dermal condensation in early buds. As can be seen in the bottom panel (Fig. 4C): when some cells were labeled in the putative feather bud, they were able to migrate into the interbud region. We think this mixing is facilitated by inhibition of p-ERK. This cell mixing does not occur in later feather buds, as the boundary between bud and interbud become stabilized.

p-ERK activity is downstream to epithelial FGF4

In order to discover molecules that may be upstream to p-ERK, we tested several growth factors (FGFs and EGFs) which may activate receptor tyrosine kinase. For example, FGF4-coated beads were implanted on stage 31 skin explants. FGF4 was used because it is expressed in the bud and known to induce feather buds (Widelitz et al., 1996). Four hours later, a large zone (2 mm in diameter) of p-ERK was induced around the bead (Fig. 5A). In controls, normal p-ERK expression remains in each bud domain. When FGF10-coated (100 μg/ml) beads were placed on stage 31 skin explants, a zone expressing comparable levels of p-ERK, as seen in feather buds, is also induced (Fig. 5A). When FGF 4 and FGF 10 beads were implanted side by side, the p-ERK-expressing region was enlarged. However, regions under the influence of both FGFs do not appear to express more p-ERK, suggesting that the two FGFs share the same pathway. p-ERK expression is also reduced in the region immediately outside of this zone, presumably because the majority of dermal cells in this region, which normally would contribute to feather buds, were instead recruited to the bead source of high FGF/p-ERK activity. These data suggest that the FGF/Raf/p-ERK pathway is involved in the feather periodic patterning process.

We then examined the effects of an FGF4-coated bead on dermal condensation formation using visible light captured by time lapse video microscopy (5 min per frame) for 10 h (Fig. 5B, Movie 5). By 10 h, a dermal condensation had formed around the FGF4 bead. The condensation continued to grow through 20 h but remained at the same size through 30 h (Fig. 5B and data not shown).

To explore the role of FGF4 as a chemo-attractant, 1% of the dissociated mesenchymal cells were labeled with Vybrant CFDA SD (Invitrogen, Carlsbad, CA) and plated at a density of 1×10^5 cells/10 μl. Heparin beads were placed in 3 μl of an FGF4 solution (100 μg/ml) for 1 h at 4 °C. The FGF-coated beads then were placed on top of plated cells. The migration of cells towards the bead was seen as the accumulation of fluorescent cells around the beads by 26 h (Fig. 5C). Cells did not accumulate around control heparin beads. The graph summarizing 5 separate experiments shows that significantly more cells accumulated around the FGF4-coated beads (location 1 — red) than at distances progressively further from the bead (locations 2 — green and 3 — blue, respectively; Fig. 5C′).

p-ERK expression in the mesenchyme is epithelium-dependent. We tested whether FGF4-coated beads can substitute for the effect of the epithelium on denuded mesenchyme by removing part of the epithelium from a skin explant (Fig. 5D). An FGF4-coated bead placed on denuded mesenchyme was able to induce mesenchymal cells around the bead to form condensations. Thus, there is a partial rescue of condensation formation. In the presence of U0126, distinct condensations towards the bead are suppressed and the dense mesenchyme appears as anastomosing cords. These results suggest that FGF4 induces p-ERK activity in the mesenchyme, causing mesenchymal cells to migrate towards areas with high FGF4 concentration and accumulate there, forming distinct condensations.

Mathematical simulation of cell behavior in the chemotactic stage of periodic patterning

In earlier work, we discussed the role of a reaction–diffusion mechanism in establishing the feather pattern (Jung et al., 1998). Here we focus on the role of chemotaxis in expanding feather primordial signaling centers during early feather bud formation. To further understand our results described above we developed a simple mathematical model based on the chemotactic response of cells to FGF4 (Fig. 6). We hypothesize that, in line with experimental observations, spot or stripe patterns in cell density are formed from an initially uniform field of mesenchymal cells by directed cell migration. We assume that cell motility becomes directed in such a way that cells move up gradients in chemo-attractant (FGF4) concentration *i.e.* chemotaxis. We further assume that cells produce the chemo-attractant, which itself undergoes random diffusion and is removed via decay or by endogenous antagonists or inhibitors of the relevant signaling pathway. The model can be summarized using the following "word" equations. More details of the mathematical model are provided in the Supplementary information.

Chemical equation

Rate of change of chemical concentration = random diffusion + chemical production − chemical decay / removal.

Cell equation

Rate of change of cell density = random motion + directed motion (chemotaxis).

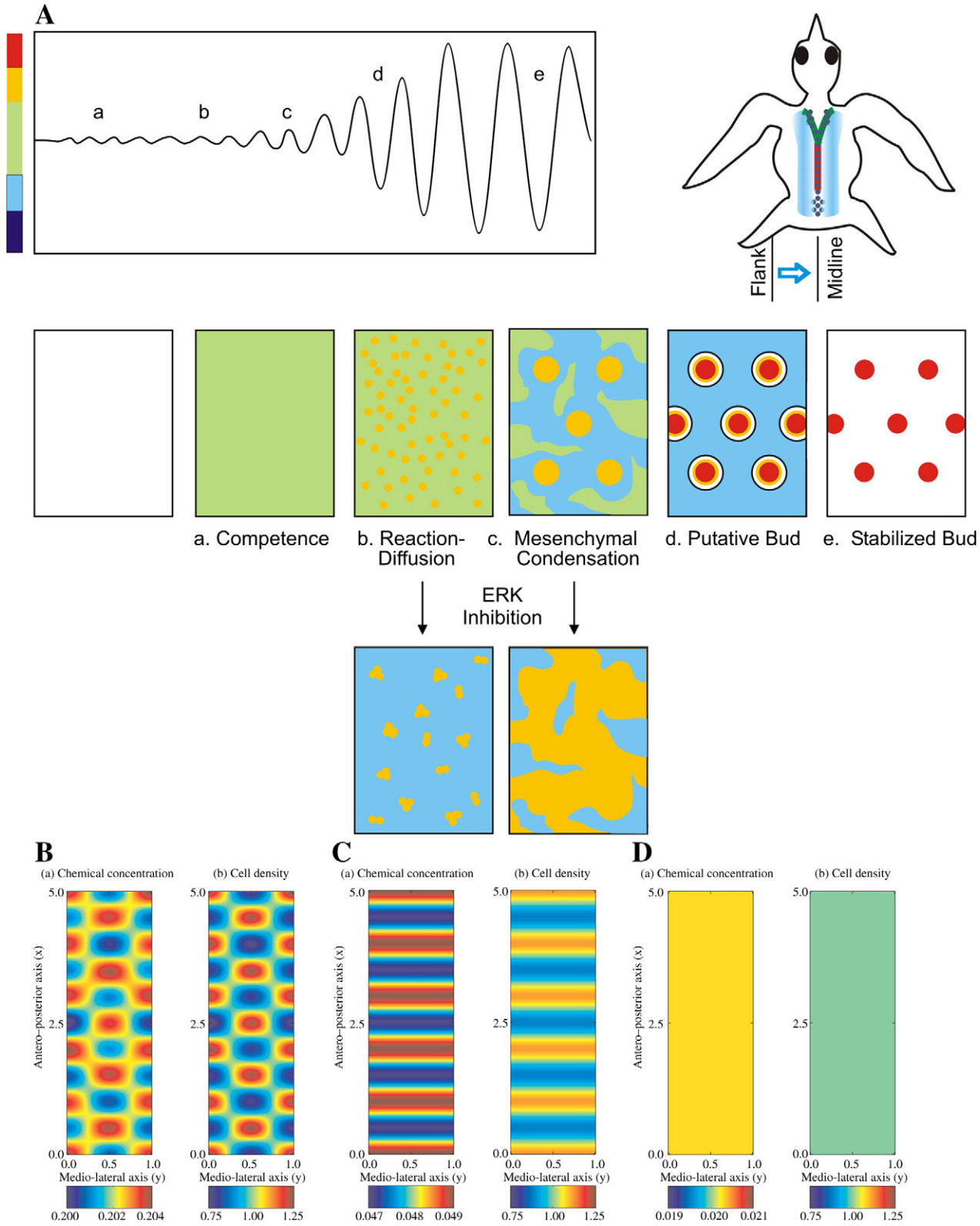

Fig. 6. Simulated model of periodic pattern formation for skin appendages. (A) Top left, schematic drawings showing the gradual specification of transition from competent basal state to the bud and the interbud state during the periodic patterning process. Top right, a schematic bird with the temporal sequence of bud formation shown to the right. Going from early to late, we have the posterior midline (red), anterior midline (green) and flank region (blue). a–e, Time course of feather pattern formation. Although the process is continuous, five stages are shown as representatives: a, competent stage; b, reaction–diffusion stage; c, mesenchymal condensation stage; d, putative primordia stage; e, stabilized bud stage. Reduction of p-ERK activity suppresses the process of dermal condensation and leads stem cells to form a different spacing pattern. Color bar represents cell density consistent with that for panels B–D. (B)–(D) Numerical simulations of the mathematical model shown in the Supplementary information. Accompanying Movies 6–8 can also be found in the Supplementary information. (B) Control model shows spatial oscillations occurring along both medio-lateral and anterior–posterior axes, resulting in spots of high cell density. Compare with Movie 6. (C) Increased chemo-attractant removal makes oscillations impossible along the medio-lateral axis. A pattern of horizontal stripes forms with cell density between the competent and bud states. Compare with Movie 7. (D) When chemo-attractant activity is further reduced by removal or antagonism, oscillations are no longer possible along either axis and the field remains homogeneous, with cell density close to that of the basal state. Compare with Movie 8. In each panel, the left is chemical concentration, and the right is cell density.

Intuitively, the model works as follows: small random fluctuations in chemo-attractant concentration or cell density are amplified by a feedback loop of chemo-attractant production and cell movement. For example, a small peak in chemo-attractant concentration causes cells to move preferentially in the direction of the peak, where chemo-attractant production increases (due to increased cell density). "Positive feedback" competition between neighboring peaks results in a pattern of cell density. Some peaks are eliminated while others are later stabilized to become dermal condensations. We define three major states as a competent basal state, a bud state, and an interbud state (Fig. 6B). The competent state is homogeneous. "Spot patterns" represent the conversion from a competent state to an oscillating bud and interbud state. "Stripe patterns" represent the one-dimensional waning of the oscillations to reach a plateaued state that lies somewhere between the competent and interbud states.

Using numerical tools we simulated the patterns in cell densities that arise via the model. Fig. 6C shows a control case: the resulting pattern along the primary row is spots of high cell density, which represent the bud state, interspersed with regions of low cell density, which represent the interbud state. The effect of perturbing p-ERK activity, as described earlier, can be tested using this model by varying the rate at which the chemo-attractant is removed. Fig. 6D shows the result of increasing the rate of chemo-attractant removal: oscillations in the medio-lateral direction gradually disappear, leading to horizontal stripes with cell density lying in a state between the basal and bud states. Fig. 6E shows the result as the removal rate is increased even further: the feather field remains in the homogeneous state. Computer simulations of the processes are shown in the Supplementary information as movies 6–8. The results of the mathematical model are consistent with those observed experimentally and support the hypothesis that p-ERK-dependent cell chemotaxis is involved in the periodic patterning of feather buds.

Discussion

In this work we use an experimentally manipulatable patterning model in which cells evolve from a homogeneous state (basal state) into a periodic array of elements arranged with different size, shape and spacing (Fig. 1A). We found that p-ERK-dependent chemotaxis is essential for the successful formation of feather patterns, suggesting this process may work alongside or in sequence with a reaction–diffusion mechanism (Fig. 7B). Another unique feature of this model is that there are two components, epithelia and mesenchyme, in this patterning process. We found that the successful patterning process requires cooperation of epithelium and mesenchyme, with molecular signals coming from one component or the other, thus demonstrating the essence of tissue interactions (Fig. 7A). An earlier study blocked FGF activity completely by delivering an FGF dominant receptor to early developing skin that suppressed bud formation (Mandler and Neubuser, 2004). While it demonstrates the essentialness of FGF activity, it is informative to study the time course of pattern formation as the whole process is inhibited. Here we adjusted the level of p-ERK activity during later stages of feather morphogenesis and by doing so, revealed the pleomorphic patterns generated at different developmental times when the dermal condensation process is blocked. Analyses of these results with time lapse movies and mathematical modeling provide new insights for understanding the process of feather pattern formation.

FGF4/ERK activity regulates the chemotactic process of mesenchymal condensations

Previously, we and others explored the role of FGFs as activators of feather formation (Jung et al., 1998; Song et al., 1996, 2004; Widelitz et al., 1996). We proposed that FGF works in conjunction with inhibitors (*i.e.*, BMPs; Jung et al., 1998; Noramly and Morgan, 1998) through a reaction–diffusion mechanism to establish feather pattern formation (Jung et al., 1998). Here we further explore the role of FGFs functioning as a chemo-attractant at a later feather morphogenesis phase. The FGF pathway belongs to the receptor tyrosine kinase (RTK) signaling family. RTK signaling can activate different downstream effectors including the MAPK/ERK pathway, the phosphatidylinositol 3 kinase (PI3K) pathway, or the phospholipase Cr (PLCr) signaling pathway. The phospholipase C inhibitor, U73122, has no effect on feather pattern formation (our unpublished data). Inhibition of PI3K affects feather bud outgrowth but does not affect the expansion of feather primordia (Atit et al., 2003). Here we focus on the MAPK/ERK signaling pathway. We show that inhibiting this pathway at different stages produces stripes of intermediate cell density, rather than clear-cut bud or interbud fates. Analyses of these stripes showed that feather placode markers, such as Shh (Ting-Berreth and Chuong, 1996a), remain diffusely distributed. Bud growth is retarded and buds fail to express differentiation markers. Surprisingly, EGF, another growth factor which functions through a tyrosine kinase receptor, does not invoke this pathway in feathers (Attit et al., 2003).

Cell tracing and time lapse movies show that in early feather morphogenesis, the ERK pathway affects the process of mesenchymal dermal condensation. Further support comes from the diffuse presence of the dermal condensation marker NCAM (Jiang and Chuong, 1992) in ERK-suppressed specimens. This parallels the involvement of growth factors in regulating adhesion molecules during limb morphogenesis (Hentschel et al., 2004; Kiskowski et al., 2004). Using a localized bead source, we showed that FGF4 can specifically induce phosphorylation of ERK. In the absence of epithelium, mesenchymal cells move randomly and cannot form discrete, spot-like dermal condensations. FGF4-coated beads placed on denuded mesenchyme rescued dermal condensation formation around the FGF source. This rescue can be neutralized by an inhibitor of ERK phosphorylation. Epithelial–mesenchymal recombination showed that the ERK inhibitor effect is mediated mainly through the mesenchyme. Consistent with these findings, FGF4 is produced by the epithelium and FGFR1 is present in the feather bud mesenchyme (Jung et al., 1998; Noji et al., 1993). These data support the notion that the FGF/FGFR/RAF/ERK pathway is involved in mediating epithelial–mesenchymal interactions with FGF from the epithelial placode binding FGFR in the mesenchyme leading to downstream events. This does not rule out an effect of FGF activity on the epithelium, which then affects mesenchyme indirectly. Previously we showed that TGFβ 2 and Shh mediate the epithelial effect on dermal condensation formation (Ting-Berreth and Chuong, 1996a,b). The relationship between TGFβ 2, Shh and FGF4 in the induction of dermal condensation remains to be investigated.

We believe that short-range activation, long-range inhibition is involved in forming microaggregates during the early stages of feather patterning, and many different classes of molecules may be involved in this process as activators or inhibitors (growth factors and their antagonists, signaling molecules, adhesion molecules). However, what matters for the patterning is the summed activity of activators or inhibitors. In line with this view, recently, based on the counteracting roles of BMP7 and BMP2 in chicken skin, a model involving cell migration and cell adhesion was proposed as underlying dermal condensation formation during feather morphogenesis (Michon et al., 2008). Whereas BMP7 induced cell migration in these studies, BMP2 induced integrin α4 and altered the splicing of fibronectin to exclude the fibronectin EIIIA domain, decrease migration and foster intracellular adhesion within the forming placode. Based on these observations, Michon et al. presented a simulation of the process of feather bud formation. Whilst their model can explain a number of experimentally observed phenomena, such as the appearance of a "zone of inhibition" around an FGF4-coated bead, it cannot explain the feather bud fusions we observe in this work.

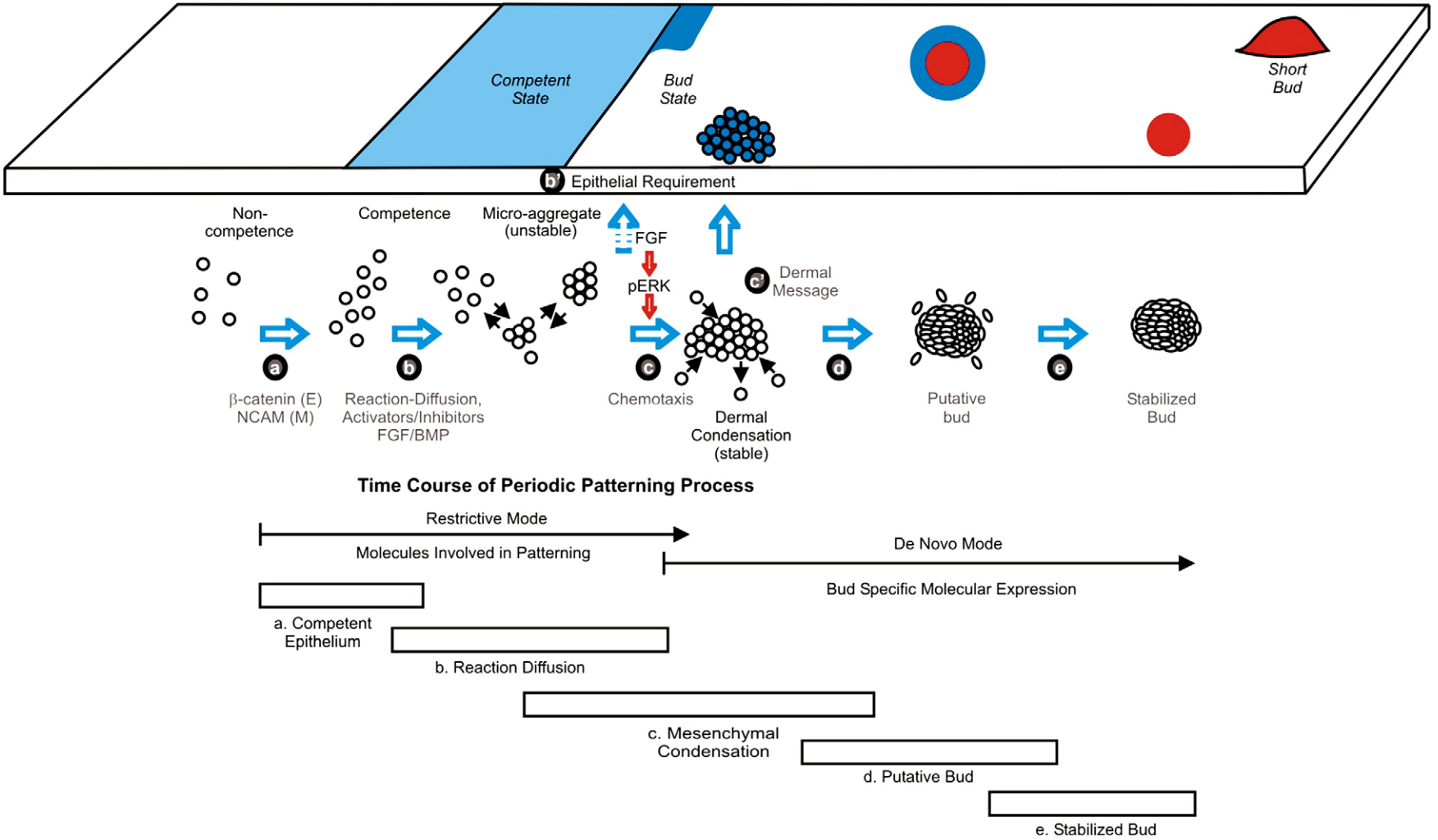

Fig. 7. Schematic summary showing the periodic patterning process during feather morphogenesis. Signaling between the mesenchyme and epithelium promotes the formation of competent epithelium. Spatially distributed activators and inhibitors of feather formation promote the expression of adhesion molecules which leads to the formation of unstable microaggregates. In these early stages, FGF acts as an activator while BMP acts as an inhibitor. The expression of FGF/p-ERK later promotes chemotaxis toward a signaling center in this patterning process leading to the formation of stable epithelial placodes and dermal condensations. The placode boundary is unstable at first but then becomes stabilized. The relative timing of molecular (restrictive versus *de novo* mode) and cellular events (5 stages) is illustrated. Please see text in discussion.

Pleomorphic patterning of stem cells

It appears that a moderate basal level of β-catenin marks the basal state of epithelia in the morphogenetic field, with competence to become either bud or interbud. Through the patterning process, this homogeneous field breaks into regions of high and low β-catenin expression levels. If a localized region with high levels of β-catenin occurs then feather buds form (state A; Noramly et al., 1999; Widelitz et al., 2000). If a region becomes deficient in β-catenin, it assumes the interbud fate (state B). Do the stripes observed here represent the basal, bud or interbud states? The stripe epithelium can express the placode marker, Shh, so it is not in the interbud state. On the other hand, Shh expressing cells are diffusely distributed all over the stripes, and the stripe cannot grow in height (*i.e.*, it fails to form a localized growth zone), nor express feather keratin (*i.e.*, it fails to differentiate). Therefore, the stripe cannot be considered as in the bud state either. Mesenchyme under the stripe expresses NCAM diffusely. Proliferation normally occurs in periodically arranged localized growth zones in bud regions, but the stripe exhibits unpatterned proliferation. By tracing the dynamics of DiI labeled mesenchyme cells, cell motility was random and active at first. Gradually, cells move towards dermal condensations where they become more adhesive and stationery. In U0126-treated specimens, mesenchymal cell motility remains high and discrete dermal condensations fail to form. Cell density in the stripes is higher than that of the interbud regions, but lower than that of the bud regions. Thus the stripe we study here has a property between the original basal state and the bud state (Fig. 6A).

We propose that an organ field in the embryo represents a multipotential status, competent to form different cell types in that organ. Through differentiation and patterning, these precursor cells are specified simultaneously or sequentially to build the topological order of the tissue. If the patterning process is altered, differentiated cells can be distributed in different configurations, in spots or stripes, consisting of a spectrum of differentiation states (Fig. 1A). Thus cells with a homogeneous stem cell status can give rise to pleomorphic patterns, depending on local signaling cues. Recently, it was shown that Wnt and DKK may also work as Turing activator–inhibitor pairs during the formation of hair germs (Sick et al., 2006; Maini et al., 2006). In accordance with the pleomorphic patterning concept here, forced expression of β-catenin resulted in a failure of the periodic patterning process, leading to the randomization of placode size and spacing, forming giant placode-like structures. These giant "placodes" exhibit differentiation markers intermediate to epidermis and hair follicle keratinocytes (Närhi et al., 2008; Zhang et al., 2008). Such results are consistent with the pleomorphic patterning concept here.

A generic cellular behavior model for a two-component periodic patterning process

Combining knowledge from our current and previous results (Jiang et al., 1999) and using FGF/p-ERK signaling as an example, we envision the following epithelial–mesenchymal interactions taking place during the patterning process (Figs. 6A and 7A). (a) *Competence stage*. The epithelium and mesenchyme gain competence when a feather tract field forms. (b) *Reaction–diffusion stage*. In this competent state, cells exhibit basal adhesiveness and random motility. Interactions occur and unstable microaggregates form. These microaggregates are only capable of eliciting a weak signal. (b′) *Dermal–epidermal signaling*. Since FGFs are produced in the epithelium, and FGFR1 is present in the mesenchyme, it is possible that microaggregates may induce the epithelia above to express more FGF, helping to create a larger signaling center that would elicit a greater signal. The molecular nature of this signal is still undergoing investigation. p-ERK expression is homogenous (Fig. 1C, flank regions in the left panels). (c) *Dermal condensation stage*. Mesenchymal p-ERK is induced in the mesenchyme beneath the epithelia with higher FGF, and its activity induces chemotaxis of mesenchymal cells, initiating the uneven distribution of cell density within the dermis. p-ERK positive primordia start to emerge at the junction of homogenously stained and distinct bud regions (Fig. 1C, left panels). (d) *Putative primordia stage*. The increasing size of dermal condensations further induces the overlying epithelia to express higher levels of FGF, which induces more p-ERK in the mesenchyme, and bigger dermal condensations. We called this "putative" because we know the placodes at this stage are unstable (Fig. 4D) and can be reset (Chuong et al., 1996; Jiang et al., 1999). p-ERK staining shows moderate levels in the putative primordia with a blurred margin. The center regions show higher expression levels that are expanding (Fig. 1C′, left and central panels). (E) *Stabilized bud stage*. The positive feedback loops continue until each dermal condensation/placode is stabilized. Thus the fates of feather bud and interbud states are established in both epithelia and mesenchyme. p-ERK is now strongly expressed in the bud but excluded from the interbud region, forming a sharp boundary (Fig. 1C′, right panel). Our model focuses on the mesenchyme. We think that the mesenchymal message is received and interpreted by the overlying epithelium which causes epithelial cell rearrangements. Although we have focused on the role of ERK in patterning the mesenchyme, we cannot rule out a role for intraepithelial signaling which is the subject of current investigations ongoing in our laboratory.

Based on these results, we develop a generic model that will not only be applicable to skin appendage formation, but also can be applied to understand how stem cells are patterned in general. We propose a mathematical model to aid in understanding the periodic patterning process. In early stages, the short-range activation, long-range inhibition is the major mechanism patterning the mesenchyme. This process is epithelial-independent, *i.e.* it can occur in the absence of epithelia (Jung et al., 1998; Jiang et al., 1999). During later stages, chemotactic cell migration towards micro-signaling centers is converted into larger stable dermal condensations. During this process, some original microaggregates will merge to become bigger or disappear, due to the phenomenon of peak competition inherent in chemotaxis. These two stages transit gradually without a sharp time boundary and will largely overlap in time (Fig. 7B) although further evidence would have to be demonstrated through future video time lapse cinematography experiments. The process is epithelial-dependent and here we show that this epithelial–mesenchymal interactive patterning process involves the expression of FGF by the epithelia and the phosphorylation of ERK in the mesenchyma.

Besides identifying the molecular members essential for feather formation, we aim to understand how the number, size and arrangement of feather primordia are determined. To this end, we developed a mathematical model based on the ability of cells to migrate toward chemo-attractants which promote bud formation as a way of testing our experimental hypothesis. Our model was able to predict the characteristic "spotted" patterns of cell density observed in control embryos and, further, to predict the effects of p-ERK perturbation. It can also be used to predict the effects of other possible chemo-attractants and their antagonists. Increasing the rate of chemo-attractant removal may produce "striped" patterns with cell density lying between the bud and interbud states.

We acknowledge that there are other mechanisms that can lead to the formation of patterning in biology. The formation of somites (spot) from presomitic mesoderm (stripe) involves oscillating expression levels of FGF, p-ERK, HES1 and Wnt (Delfini et al., 2005). In limb bud micromass cultures, local activation coupled with lateral inhibition is proposed to be important for the formation of cartilage nodules (Newman and Bhat, 2007). It is tempting to propose some unifying fundamental mechanism may underlie these periodic patterning processes. More studies that combine experimental and theoretical approaches will be required for us to further understand the essence of biological pattern formation (Chuong and Richardson, 2009).

Experimental procedures

Embryos, skin explant culture and recombination

Specific pathogen-free (SPF) White Leghorn chick embryos were obtained from Charles River Laboratories (Preston, CT, USA) and staged according to Hamburger and Hamilton (H&H) (1951). Explant cultures, partial removal of epithelia and bead preparations were performed as described (Ting-Berreth and Chuong, 1996b). Application of the inhibitor, U0126 (Sigma, St. Louis, MO, USA), to chicken skin explant cultures was achieved by supplementation of the growth media. U0126 was dissolved in DMSO and added to a final concentration of 10 μg/ml. This concentration was optimized in preliminary studies within the laboratory. Control cultures were supplemented with an equivalent volume of DMSO.

In situ hybridization and immunohistochemistry

Procedures were performed as described (Jiang and Chuong, 1992; Ting-Berreth and Chuong, 1996a). The automated Discovery *in situ* hybridization unit from Ventana was used for some specimens.

Electroporation, probe and siRNA preparation

The ERK-siRNA sense sequence is AGA UCU UAC UGC GCU UCA GTT and antisense sequence is CUG AAG CGC AGU AAG AUC UTT. The target oligonucleotide was suspended in DEPC-water at a concentration of 50 μM. The ERK-siRNA oligonucleotides were annealed with 5X annealing buffer (250 mM Tris–HCl, pH 7.5, 500 mM NaCl, DEPC-water) for 2 min at 95 °C and allowed to cool to room temperature. siRNA-ERK was diluted in electroporation hypo-osmolar buffer (eppendorf) 5 μM and RFP added as a marker to visualize affected sites by electroporation. E31 chicken skin was electroporated with an siRNA-ERK mixture in which the negative pole faces the epithelium. The electric current was delivered as 3 pulse of 5v/50 ms. After electroporation, the skin was cultured on 60 mm culture inserts (Falcon, San Jose, CA, USA) for 2 days. The electroporation efficiency was checked by florescence microscopy. The ERK-siRNA explants have reduced feather bud elongation. The feather buds were partially inhibited by ERK-siRNA.

Cell labeling

To observe cell migration towards an FGF4 coated bead, 1% of the dissociated mesenchymal cells isolated from stage 31 skin explants were labeled with Vybrant CFDA SE Cell Tracer (10 mM; Invitrogen, Carlsbad, CA, USA) for 15 min at 37 °C and washed with media for 30 min at 37 °C following the manufacturer's recommended protocol. The labeled cells were then mixed with unlabeled cells and 1×10^5 cells were plated in 10 μl on a culture insert (Falcon, San Jose, CA, USA). For lineage tracing cells in skin explants were microinjected with 1–5 nl of 0.1% DiI in 70% ethanol (Invitrogen, Carlsbad, CA, USA) via glass capillaries followed by two washes with PBS. The labeled skin explants were cultured for 72 h. The results were visualized by fluorescent microscopy.

Time lapse video microscopy

Skin explants were grown on 60 mm culture inserts (Falcon, San Jose, CA, USA) in a SmartSlide environmental chamber (Wafergen Biosystems, Fremont, CA, USA) which maintained temperature and CO_2 conditions. Time lapse photographs were obtained every 5 min through an Olympus IMT-2 microscope.

Quantification of cell density

Mesenchymal cell density was calculated in feather buds and interbud regions in control specimens. The cells found within three feather buds and interbuds were counted and cell density was calculated by dividing the total size of the bud and interbud regions (μm^2). The mesenchymal cells from three fused skin samples were counted and cell density was calculated by dividing by the size of the fused area (μm^2).

Disclosure

Widelitz serves on the advisory board to Wafergen Biosystems.

Acknowledgments

We are grateful for grant support from NIAMS AR2177, AR47364 (CMC), and AR052397 (RW). REB would like to thank Microsoft Research for a European Postdoctoral Research Fellowship, Research Councils UK for an RCUK Academic Fellowship in Mathematical Biology and St Hugh's College, Oxford for a Junior Research Fellowship. REB also gratefully acknowledges support from the Astor Travel Fund at the University of Oxford in order to visit the University of Southern California. PKM was partially supported by a Royal Society Wolfson Merit Award. Some photos use microscopes from the microscopy sub core at the USC Center for liver diseases (NIH 1 P30 DK48522).

Accession number: Raf-1 accession number NM205307.

Appendix A. Supplementary data

Supplementary data associated with this article can be found, in the online version, at doi:10.1016/j.ydbio.2009.07.036.

References

Atit, R., Conlon, R.A., Niswander, L., 2003. EGF signaling patterns the feather array by promoting the interbud fate. Dev. Cell 4, 231–240.
Ball, P., 1999. The self-made Tapestry: Pattern Formation in Nature. Oxford University Press, New York.
Cabernard, C., Affolter, M., 2005. Distinct roles for two receptor tyrosine kinases in epithelial branching morphogenesis in Drosophila. Dev. Cell 9, 831–842.
Chang, C.H., Jiang, T.X., Lin, C.M., Burrus, L.W., Chuong, C.M., Widelitz, R., 2004. Distinct Wnt members regulate the hierarchical morphogenesis of skin regions (spinal tract) and individual feathers. Mech. Dev. 121, 157–171.
Chen, C.W., Chuong, C.M., 2000. Dynamic expression of lunatic fringe during feather morphogenesis: a switch from medial–lateral to anterior–posterior asymmetry. Mech. Dev. 91, 351–354.
Christley, S., Alber, M.S., Newman, S.A., 2007. Patterns of mesenchymal condensation in a multiscale, discrete stochastic model. PLoS Comput. Biol. 3, e76.
Chuong, C.M., Richardson, M.R., 2009. Pattern formation. Int. J. Dev. Biol. 53, 653–659.
Chuong, C.-M., Ting-Berreth, S., Widelitz, R.B., Jiang, T.-X., 1996. Early events during the regeneration of skin appendages: order of molecular reappearance following epithelial–mesenchymal recombination with rotation. J. Invest. Dermatol. 107, 639–646.
Chuong, C.-M., Wu, P., Plikus, M.V., Jiang, T.X., Widelitz, R.B., 2006. Engineering stem cells into organs: topobiological transformations demonstrated by beak, feather and other ectodermal organ morphogenesis. Curr. Top. Dev. Biol. 72, 237–274.
Crowe, R., Henrique, D., Ish-Horowicz, D., Niswander, L., 1998. A new role for Notch and Delta in cell fate decisions: patterning the feather array. Development 125, 767–775.
Delfini, M.C., Dubrulle, J., Malapert, P., Chal, J., Pourquie, O., 2005. Control of the segmentation process by graded MAPK/ERK activation in the chick embryo. Proc. Natl. Acad. Sci. U. S. A. 102, 11343–11348.
Dequéant, M.L., Pourquié, O., 2008. Segmental patterning of the vertebrate embryonic axis. Nat. Rev., Genet. 9, 370–382.
Drew, C.F., Lin, C.M., Jiang, T.X., Blunt, G., Mou, C., Chuong, C.M., Headon, D.J., 2007. The Edar subfamily in feather placode formation. Dev. Biol. 305, 232–245.
Fisher, C.E., Michael, L., Barnett, M.W., Davies, J.A., 2001. Erk MAP kinase regulates branching morphogenesis in the developing mouse kidney. Development 128, 4329–4338.
Hamburger, V., Hamilton, H.L., 1951. A series of normal stages in the development of the chick embryo. J. Morphol. 88, 49–92.
Harris, M.P., Williamson, S., Fallon, J.F., Meinhardt, H., Prum, R.O., 2005. Molecular evidence for an activator–inhibitor mechanism in development of embryonic feather branching. Proc. Natl. Acad. Sci. U. S. A. 102, 11734–11739.
Hentschel, H.G., Glimm, T., Glazier, J.A., Newman, S.A., 2004. Dynamical mechanisms for skeletal pattern formation in the vertebrate limb. Proc. Biol. Sci. 271, 1713–1722.
Jiang, T.X., Chuong, C.M., 1992. Mechanism of skin morphogenesis. I. Analyses with antibodies to adhesion molecules tenascin, N-CAM, and integrin. Dev. Biol. 150, 82–98.

Jiang, T.-X., Jung, H.-S., Widelitz, R.B., Chuong, C.-M., 1999. Self organization is the initial event in periodic feather patterning: roles of signaling molecules and adhesion molecules. Development 126, 4997–5009.
Jiang, T.X., Widelitz, R.B., Shen, W.M., Will, P., Wu, D.Y., Lin, C.M., Jung, H.S., Chuong, C.M., 2004. Integument pattern formation involves genetic and epigenetic controls: feather arrays simulated by digital hormone models. Int. J. Dev. Biol. 48, 117–135.
Jung, H.-S., Francis-West, P.H., Widelitz, R.B., Jiang, T.-X., Ting-Berreth, S., Tickle, C., Wolpert, L., Choung, C.-M., 1998. Local inhibitory action of BMPs and their relationships with activators in feather formation: implications for periodic patterning. Dev. Biol. 196, 11–23.
Keller, G., 2005. Embryonic stem cell differentiation: emergence of a new era in biology and medicine. Genes Dev. 19, 1129–1155.
Kiskowski, M.A., Alber, M.S., Thomas, G.L., Glazier, J.A., Bronstein, N.B., Pu, J., Newman, S.A., 2004. Interplay between activator–inhibitor coupling and cell–matrix adhesion in a cellular automaton model for chondrogenic patterning. Dev. Biol. 271, 372–387.
Kondo, S., 2002. The reaction–diffusion system: a mechanism for autonomous pattern formation in the animal skin. Genes Cells 7, 535–541.
Lin, C.M., Jiang, T.X., Widelitz, R.B., Chuong, C.M., 2006. Molecular signaling in feather morphogenesis. Curr. Opin. Cell Biol. 18, 730–741.
Liu, R.T., Liaw, S.S., Maini, P.K., 2006. Two-stage Turing model for generating pigment patterns on the leopard and the jaguar. Phys. Rev., E Stat. Nonlinear Soft Matter Phys. 74, 011914–1–011914-8.
Maini, P.K., Baker, R.E., Chuong, C.M., 2006. The Turing model comes of molecular age. Science 314, 1397–1398.
Mandler, M., Neubuser, A., 2004. FGF signaling is required for initiation of feather placode development. Development 131, 3333–3343.
Matsubayashi, Y., Ebisuya, M., Honjoh, S., Nishida, E., 2004. ERK activation propagates in epithelial cell sheets and regulates their migration during wound healing. Curr. Biol. 14, 731–735.
Meinhardt, H., Gierer, A., 2000. Pattern formation by local self-activation and lateral inhibition. BioEssays 22, 753–760.
Michon, F., Forest, L., Collomb, E., Demongeot, J., Dhouailly, D., 2008. BMP2 and BMP7 play antagonistic roles in feather induction. Development 135, 2797–2805.
Miura, T., Maini, P.K., 2004. Speed of pattern appearance in reaction–diffusion models: implications in the pattern formation of limb bud mesenchyme cells. Bull. Math. Biol. 66, 627–649.
Murray, J.D., 2003. Mathematical Biology II: Spatial Models and Biomedical Applications. Springer-Verlag, New York.
Myerscough, M.R., Murray, J.D., 1991. Pigmentation pattern formation on snakes. J. Theor. Biol. 149, 339–360.
Nagorcka, B.N., Mooney, J.R., 1992. From stripes to spots: prepatterns which can be produced in the skin by a reaction–diffusion system. IMA J. Math. Appl. Med. Biol. 9, 249–267.
Närhi, K., Järvinen, E., Birchmeier, W., Taketo, M.M., Mikkola, M.L., Thesleff, I., 2008. Sustained epithelial β-catenin activity induces precocious hair development but disrupts hair follicle down-growth and hair shaft formation. Development 135, 1019–1028.
Newman, S.A., Comper, W.D., 1990. 'Generic' physical mechanisms of morphogenesis and pattern formation. Development 110, 1–18.
Newman, S.A., Bhat, R., 2007. Activator–inhibitor dynamics of vertebrate limb pattern formation. Birth Defects Res. C Embryo Today 81, 305–319.
Newman, S.A., Christley, S., Glimm, T., Hentschel, H.G., Kazmierczak, B., Zhang, Y.T., Zhu, J., Alber, M., 2008. Multiscale models for vertebrate limb development. Curr. Top. Dev. Biol. 81, 311–340.
Noji, S., Koyama, E., Myokai, F., Nohno, T., Ohuchi, H., Nishikawa, K., Taniguchi, S., 1993. Differential expression of three chick FGF receptor genes, FGFR1, FGFR2 and FGFR3, in limb and feather development. Prog. Clin. Biol. Res. 383B, 645–654.
Noramly, S., Morgan, B.A., 1998. BMPs mediate lateral inhibition at successive stages in feather tract development. Development 125, 3775–3787.
Noramly, S., Freeman, A., Morgan, B.A., 1999. β-catenin signaling can initiate feather bud development. Development 126, 3509–3521.
Painter, K.J., Maini, P.K., Othmer, H.G., 1999. Stripe formation in juvenile Pomacanthus explained by a generalized Turing mechanism with chemotaxis. Proc. Natl. Acad. Sci. U. S. A. 96, 5549–5554.
Patel, K., Makarenkova, H., Jung, H.-S., 1999. The role of long range, local and direct signalling molecules during chick feather bud development involving the BMP's, follistatin and the Eph receptor tyrosine kinase Eph-A4. Mech. Dev. 86, 51–62.
Pourquie, O., 2003. Vertebrate somitogenesis: a novel paradigm for animal segmentation? Int. J. Dev. Biol. 47, 597–603.
Sawada, A., Shinya, M., Jiang, Y.J., Kawakami, A., Kuroiwa, A., Takeda, H., 2001. Fgf/MAPK signalling is a crucial positional cue in somite boundary formation. Development 128, 4873–4880.
Sengel, P., 1976. Morphogenesis of skin. In: Abercrombie, M., Newth, D.R., Torrey, J.G. (Eds.), Developmental and Cell Biology Series. Cambridge Univ. Press, Cambridge.
Sick, S., Reinker, S., Timmer, J., Schlake, T., 2006. WNT and DKK determine hair follicle spacing through a reaction–diffusion mechanism. Science 314, 1447–1450.
Small, S., Levine, M., 1991. The initiation of pair-rule stripes in the Drosophila blastoderm. Curr. Opin. Genet. Dev. 1, 255–260.
Song, H., Wang, Y., Goetinck, P.F., 1996. Fibroblast growth factor 2 can replace ectodermal signaling for feather development. Proc. Natl. Acad. Sci. U. S. A. 93, 10246–10249.
Song, H.K, Lee, S.H., Goetinck, P.F., 2004. FGF-2 signaling is sufficient to induce dermal condensations during feather development. Dev. Dyn. 231, 741–749.
Tao, H., Yoshimoto, Y., Yoshioka, H., Nohno, T., Noji, S., Ohuchi, H., 2002. FGF10 is a mesenchymally derived stimulator for epidermal development in the chick embryonic skin. Mech. Dev. 116, 39–49.
Ting-Berreth, S.A., Chuong, C.-M., 1996a. Sonic Hedgehog in feather morphogenesis: induction of mesenchymal condensation and association with cell death. Dev. Dyn. 207, 157–170.
Ting-Berreth, S.A., Chuong, C.-M., 1996b. Local delivery of TGF β2 can substitute for placode epithelium to induce mesenchymal condensation during skin appendage morphogenesis. Dev. Biol. 179, 347–359.
Vasiev, B.N., Hogeweg, P., Panfilov, A.V., 1994. Simulation of *Dictyostelium discoideum* aggregation via reaction–diffusion model. Phys. Rev. Lett. 73, 3173–3176.
Viallet, J.P., Prin, F., Olivera-Martinez, I., Hirsinger, E., Pourquie, O., Dhouailly, D., 1998. Chick Delta-1 gene expression and the formation of the feather primordia. Mech. Dev. 72, 159–168.
Watt, F.M., 2001. Stem cell fate and patterning in mammalian epidermis. Curr. Opin. Genet. Dev. 11, 410–417.
Weissman, I.L., 2000. Translating stem and progenitor cell biology to the clinic: barriers and opportunities. Science 287, 1442–1446.
Widelitz, R.B., Jiang, T.-X., Noveen, A., Chen, C.-W., Chuong, C.-M., 1996. FGF induces new feather buds from developing avian skin. J. Invest. Dermatol. 107, 797–803.
Widelitz, R.B., Jiang, T.-X., Lu, J., Chuong, C.-M., 2000. Beta-catenin in epithelial morphogenesis: Conversion of part of avian foot scales into feather buds with a mutated beta-catenin. Dev. Biol. 219, 98–114.
Widelitz, R.B., Baker, R.E., Plikus, M., Lin, C.M., Maini, P.K., Paus, R., Chuong, C.M., 2006. Distinct mechanisms underlie pattern formation in the skin and skin appendages. Birth Defects Res. C Embryo Today 15, 280–291.
Wolpert, L., 1971. Positional information and pattern formation. Curr. Top. Dev. Biol. 6, 183–224.
Yu, M., Wu, P., Widelitz, R.B., Chuong, C.M., 2002. The morphogenesis of feathers. Nature 420, 308–312.
Zhang, Y., Andl, T., Yang, S.H., Teta, M., Liu, F., Seykora, J.T., Tobias, J.W., Piccolo, S., Schmidt-Ullrich, R., Nagy, A., Taketo, M.M., Dlugosz, A.A., Millar, S.E., 2008. Activation of β-catenin signaling programs embryonic epidermis to hair follicle fate. Development 135, 2161–2172.
Zorzano, M.-P., Hochberg, D., Cuevas, M.-T., Gómez-Gómez, J.-M., 2005. Reaction–diffusion model for pattern formation in *E. coli* swarming colonies with slime. Phys. Rev. E 71, 031908.